water

MDPI

Article

Myriophyllum aquaticum-Based Surface Flow Constructed Wetlands for Enhanced Eutrophic Nutrient Removal—A Case Study from Laboratory-Scale up to Pilot-Scale Constructed Wetland

Shugeng Feng [1], Shengjun Xu [1], Xupo Zhang [1], Rui Wang [1], Xiaona Ma [1], Zhirui Zhao [1,3], Guoqiang Zhuang [1,2], Zhihui Bai [1,2] and Xuliang Zhuang [1,2,*]

[1] Key Laboratory of Environmental Biotechnology, Research Center for Eco-Environmental Sciences, Chinese Academy of Sciences, Beijing 100085, China; fengshugeng@163.com (S.F.); sjxu@rcees.ac.cn (S.X.); xupozhang@foxmail.com (X.Z.); szywangrui@126.com (R.W.); 13733212151@163.com (X.M.); zhiruizh@163.com (Z.Z.); gqzhuang@rcees.ac.cn (G.Z.); zhbai@rcees.ac.cn (Z.B.)

[2] College of Resources and Environment, University of Chinese Academy of Sciences, Beijing 100049, China

[3] College of Water Resources and Environment, Hebei Geo University, Shijiazhuang 050031, China

* Correspondence: xlzhuang@rcees.ac.cn; Tel.: +86-010-6284-9193

Received: 7 August 2018; Accepted: 19 September 2018; Published: 6 October 2018

check for updates

Abstract: Water pollution caused by various eutrophic nutrients such as nitrogen (N) and phosphorus (P), such as outbreaks of eutrophication in rivers and lakes, has become a serious environmental problem in China. Such problems have spurred extensive studies aiming at finding environmentally friendly solutions. Various constructed wetlands (CWs), planted with different macrophytes, have been considered as environmentally safe technologies to treat various wastewaters for several decades. Due to their low energy and operational requirements, CWs are promising alternative solutions to water eutrophication problems. Within the CWs, macrophytes, sediments, and the microbial community are indispensable constituents of such an ecosystem. In this study, a laboratory-scale surface flow CW (LSCW) was constructed to investigate the effects of two different plants, *Eichhornia* (*E.*) *crassipes* (Mart.) Solms and *Myriophyllum* (*M.*) *aquaticum*, on the removal of eutrophic N and P. The results showed that both plants could significantly reduce these nutrients, especially ammonium (NH_4^+), and LSCW planted with *M. aquaticum* performed better (82.1% NH_4^+ removal) than that with *E. crassipes* (66.4% NH_4^+ removal). A Monod model with a plug flow pattern was used to simulate the relationship of influent and effluent concentrations with the kinetic parameters of this LSCW. Based on the model, a pilot-scale surface flow CW (PSCW) was designed, aiming to further enhance N and P removal. The treatment with *M. aquaticum* and polyethylene materials showed the best removal efficiency on NH_4^+ as well as on total nitrogen and phosphorus. In general, the enlarged PSCW can be a promising solution to the eutrophication problems occurring in aquatic environments.

Keywords: constructed wetlands; wastewater; *Myriophyllum aquaticum*; nitrogen and phosphorus removal; Monod model

1. Introduction

Water pollution caused by eutrophic N and P has become a severe environmental problem leading to shrinkage of the water environmental capacity, and has drawn broad attention in China [1,2]. The N and P contents originate from a variety of point and nonpoint sources [3–5], mainly due to rising anthropogenic activities [6,7]. Common approaches including management of domestic and industrial wastewater disposal plans and raising of wastewater treatment standards, etc., have been used to mitigate the N and P input into aquatic environments [8,9]. However, these approaches were followed by a series of problems as these measures shifted the problems to wastewater treatment plants, substantially increasing the financial, operational, and technical difficulties of wastewater treatment plants [10,11]. Due to these difficulties, wastewater treatment could not always suffice for the discharging requirement of China. Considerable amounts of N and P in the discharged effluents would therefore accumulate in rivers and lakes, leading to serious environment problems.

Facing such serious eutrophic pollution, constructed wetlands (CWs) emerged as environmentally friendly technologies simulating the natural wetlands and were broadly used in the treatment of wastewater [12,13]. The CWs could efficiently remove the pollutants in waters, including organic matter, N and P, pharmaceutical residues, and microbial pathogens, etc. [14–17]. To remove these pollutants, a series of systematical processes were correlated, such as sedimentation, precipitation, volatilization, macrophyte uptake, and various microbial metabolisms, etc.; macrophyte uptake and microbial metabolisms are thought to play the central biological roles [10,17–19].

Macrophytes used in CWs usually have superior tolerance to various pollutants (especially to those high-concentration nutrients and toxic pollutants) and have an expected capability of reducing the nutritional pollution in water [20–23]. Amongst those ubiquitously used macrophytes, *E. crassipes* and *M. aquaticum* have exhibited excellent capacity for pollutant removal because of their superior tolerance to, and efficient absorption of, N and P nutrients, as well as heavy metals, etc. [24]. However, *E. crassipes* has been found to be an exotic species without natural enemies, which will likely deteriorate the ecosystems in the long term [25]. On the contrary, the risks of *M. aquaticum* spreading into other ecosystems could be manageable [26,27].

The microbial community also plays an important role in CW ecosystems [28–31]. The functional microbial communities in CWs consist of microorganisms that can decompose the complex biomass to simpler organic carbon, and prokaryotes that can perform complete nitrification and denitrification and phosphorus removal. The mechanisms of N and P removal in CWs are similar to those that occur in wastewater treatment. For example, it was recently reported that the *Pseudomonas* species harboring polyphosphate kinase (PPK), which have been essential for microbial phosphorus removal in wastewater treatment, were tightly correlated with the total phosphorus removal in a vertical flow constructed wetland [32]. Additionally, these microbial communities, grown either as floating aggregates [33–35] or attached to various surfaces (forming biofilms), could be far more efficient in reducing these N and P nutrients than their free-swimming counterparts [35–37]. In common CWs, these communities mainly attach to plant roots and other filling materials to form mature communities, greatly enhancing the N and P removal efficiencies [36]. Therefore, filling substrates made from different materials were broadly studied for their nutrient removal efficiencies in CW ecosystems.

In order to further enhance the removal efficiency, macrophytes and microbial communities should develop in a composite system [38]. The floating bed technology was developed accordingly, providing sufficient above-water areas for macrophyte growth and submerged spaces for filling materials, such as polyethylene fiber (PF), for the attachment of microbial communities [39–41].

Inspired by previous studies [27,42], a laboratory-scale surface flow CW (LSCW) was designed aiming to determine (a) the best pollutant removal efficiencies by different treatments including *E. crassipes*, *M. aquaticum*, and PFs; (b) the optimal operational conditions for this LSCW; and (c) the closest match of removal results with the simulations of kinetic models. The simulation results showed that pollutant removal was best simulated with the Monod kinetics model combined with the plug flow pattern. Based on the simulated model, a pilot-scale surface flow CW (PSCW) was conceived to verify (d) the pollutant removal efficiencies by different treatments including *M. aquaticum*, PFs, and *M. aquaticum* combined with PFs using floating beds; and (e) the feasibility of up-scaled design of the PSCW. Both CWs showed excellent removal efficiencies of chemical oxygen demand (COD), ammonium (NH_4^+), total nitrogen (TN), and total phosphorus (TP). The performance of PSCW in NH_4^+ removal significantly exceeded the theoretical prediction, which indicated that the design of the PSCW enlarged from the LSCW was successful. In general, the PSCW system showed excellent removal capability for N and P nutrients and great potential for treating wastewater with eutrophic pollutants in high concentrations; *M. aquaticum* exhibited great potential for advanced treatment of wastewater.

2. Materials and Methods

2.1. Design and Setup of the LSCW

The design of the LSCW was adopted from previous studies with major modifications [43,44]. This LSCW was set up in a laboratory room and constructed as a U-type riverlike channel of 18 m × 0.5 m × 0.5 m in size (length by width by height, L × W × D) with polymethyl methacrylate plates (Figure 1A). One end of the channel was the inlet and the other the outlet, and 1.0 m away from each end, a water retaining plate was placed, making a treatment zone of the LSCW. The bottom of the channel was covered with soil to a 5 cm depth (Figure 1B). Four treatments were used, including treatment without plants or PFs (control, CK), treatment with PFs (PFT), with *E. crassipes* (ECT), and with *M. aquaticum* (MAT). Both *E. crassipes* and *M. aquaticum* were grown until the shoot length reached 30 cm, and then transplanted into the corresponding treatments with a density of 50 plants/m^2. Eight strands of PFs (0.3 m each) were attached under each floating plate (0.3 m × 0.3 m) for attachment of microorganisms (Figure 1B). The floating plates were placed every 0.5 m in the treatment area. In order to shorten the development of the microbial community on the PFs, communities including ammonium-oxidizing bacteria (*Acinetobacter* sp.), nitrifiers, and denitrifiers (*Rhodococcus* sp.) were first cultivated and fixed on the PFs. In brief, bacterial cells were grown to 10^9 CFU/mL and collected by centrifugation (6000 rpm, 5 min), then the pellet was re-suspended in water. Meanwhile, polyvinyl alcohol (PVA) was prepared for bacterial cell fixation on the PFs. In general, 50 g of PVA was thoroughly dissolved in 300 mL of distilled water through heating; the gel-like mixture was cooled to room temperature before being evenly mixed with the prepared bacterial cultures in equal volume. This PVA–bacteria mixture was evenly sprayed on the PFs for microbial community attachment for the subsequent experiment. The room temperature was kept at 26 ± 2 °C during the experiment, and illuminating lights (430 W, 40,000 LM) were used to provide enough light for plant growth.

A

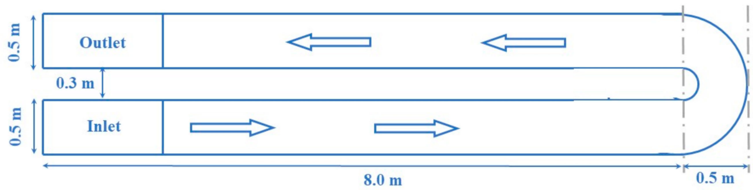

B

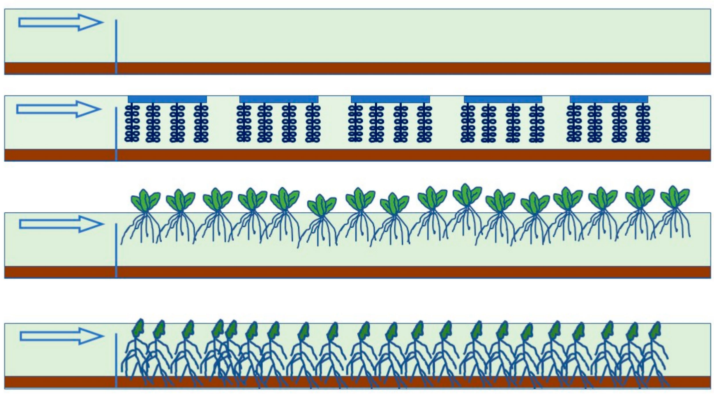

Figure 1. Schematic diagrams of the laboratory-scale surface flow constructed wetlands (LSCW). Planform (**A**) and lateral views (**B**) of the LSCW are demonstrated, and the arrow points in the flow direction. The treatments are shown from top to bottom in (**B**) as the control (CK), treatment with polyethylene fibers (PFT), with *E. crassipes* (ECT), and with *M. aquaticum* (MAT), respectively.

2.2. Determination of the Hydraulic Retention Time (HRT) of the LSCW

The management of the HRT was operated through adjusting the daily influent. Each treatment was equipped with a peristaltic pump and an input water flow meter for in situ monitoring. The effects of 4 d and 7 d HRT were determined, respectively. To reach a 7 d HRT, the influent was 0.56 m^3/d, and for 4 d HRT, the influent was increased to 0.98 m^3/d. The experiments for HRT were conducted three times, and the total experimental period spanned from 20 January to 10 April 2016.

2.3. Modelling of the LSCW and Accuracy Test of Models

To correlate the influent and effluent of pollutants in the LSCW, simplified equations adopted from previous studies were established by combing the plug flow pattern with Monod kinetics, and are expressed as follows [45]:

$$A_h = \frac{Q\left(C_{in} - C_{out} + C_{half}\ln\left(\frac{C_{in}}{C_{out}}\right)\right)}{K} \tag{1}$$

In this equation, A_h represents the surface area of the CW (m^2); Q is the daily wastewater influent ($m^3 \cdot d^{-1}$); C_{in} and C_{out} are pollutant concentrations (mg/L) of influent and effluent, respectively; and K represents the rate constant ($g \cdot m^{-2} \cdot d^{-1}$), which is derived from the maximum removal rate of the corresponding pollutant ($g \cdot m^{-3} \cdot d^{-1}$) [45]. The constant C_{half} represents the concentration of the corresponding pollutant when the pollutant removal efficiency reaches half the maximum removal rate. Based on previous studies [45–47], the removal dynamics of COD and NH_4^+ in the LSCW were used to establish the simulation models and were also used to evaluate the pollutant removal efficiency of the PSCW. The C_{half} values for COD and NH_4^+ were taken as 60 mg/L and 0.05 mg/L, respectively, which are the concentrations used for Monod equations in wastewater treatment processes [45–47]. The constants neglect the surrounding temperature effects and assume that the microbial communities in the treatments of the CWs are stable.

To generate a general form of the relationship of influent and effluent concentrations with the rate constant and surface area of the CW, Equation (1) can be transferred into the following form:

$$f(C_{in}, C_{out}) = K(A_h/Q) \tag{2}$$

Since the influent and effluent concentrations of COD and NH_4^+ in the LSCW, the HRT, the surface area of the LSCW (A_h), and the daily influent volume of water (Q) were already determined, the corresponding K values can be obtained. The geometric mean of the K values was taken to establish the kinetic Monod equations for the LSCW. With the established equations, the theoretical effluent concentrations can be obtained from the known influent concentrations and K values. The accuracy of the equations for the LSCW was assessed by comparing the theoretical concentrations with the actual CW performance, and an insignificant difference indicated their accuracy.

2.4. Design of the PSCW Enlarged from the LSCW

A pilot-scale surface flow constructed wetland was subsequently conceived with the established equations for the LSCW. The original intent for the LSCW and PSCW was the advanced treatment of effluent from wastewater treatment plants. Based on this purpose, the influent COD and NH_4^+ were set at 50 mg/L and 5 mg/L, and the effluent COD and NH_4^+ were brought to 30 mg/L and 1.5 mg/L, respectively. The enlargement of the PSCW from the LSCW was mainly achieved through increasing the influent volumes (Q), which was accompanied with the increment of the surface area (A_h). The conceived PSCW was intended to increase to 10 times the influent volume of the LSCW treatment; therefore, the required A_h for the PSCW could be obtained through the established Monod equations for the LSCW. To satisfy the removal requirement, the equations for both COD and NH_4^+

were used to calculate the required A_h for the PSCW, and the greater A_h was taken for the design of the PSCW. The A_h calculation is discussed further on.

Based on the A_h calculation, the frame structure of the LSCW, and the site conditions where the PSCW was intended to be constructed, each individual treatment unit of the PSCW was designed as a riverlike channel (40 m × 2.0 m × 1.0 m, L × W × D). Different treatments, including *M. aquaticum*, PFs, and combination of *M. aquaticum* and PFs, were adopted from the LSCW, which finally resulted in the PSCW consisting of six treatment channels (final scale of the PSCW: 40 m × 12.0 m × 1.0 m, L × W × D, Figure 2A). The construction of the PSCW also introduced a multi-treatment-stage strategy to further enhance the pollutant removal effects [48]; therefore, each treatment channel of the PSCW was evenly divided into five continuous subunits (8.0 m × 2.0 m × 1.0 m, L × W × D). The PSCW was constructed in an open field at Changsha Environmental Observation Station of the Chinese Academy of Sciences (CAS) in Hunan Province (113°20′ E, 28°34′ N).

2.5. Setup and Operational Conditions of the PSCW

Based on the above design, the PSCW was constructed with glass fiber plates consisting of 30 subunits, which made up six identical treatment channels. Each channel was watertight against the adjacent channel, and each channel had an individual inlet and outlet (Figure 2A). The subunits in each channel were connected through water-level connecting pipes (Figure 2B), so that the water could not flow into the next unit until it reached the opening of the connecting pipe. Treated water in the last unit was discharged through the connecting pipes into the neighboring advanced treatment system (not included in this study).

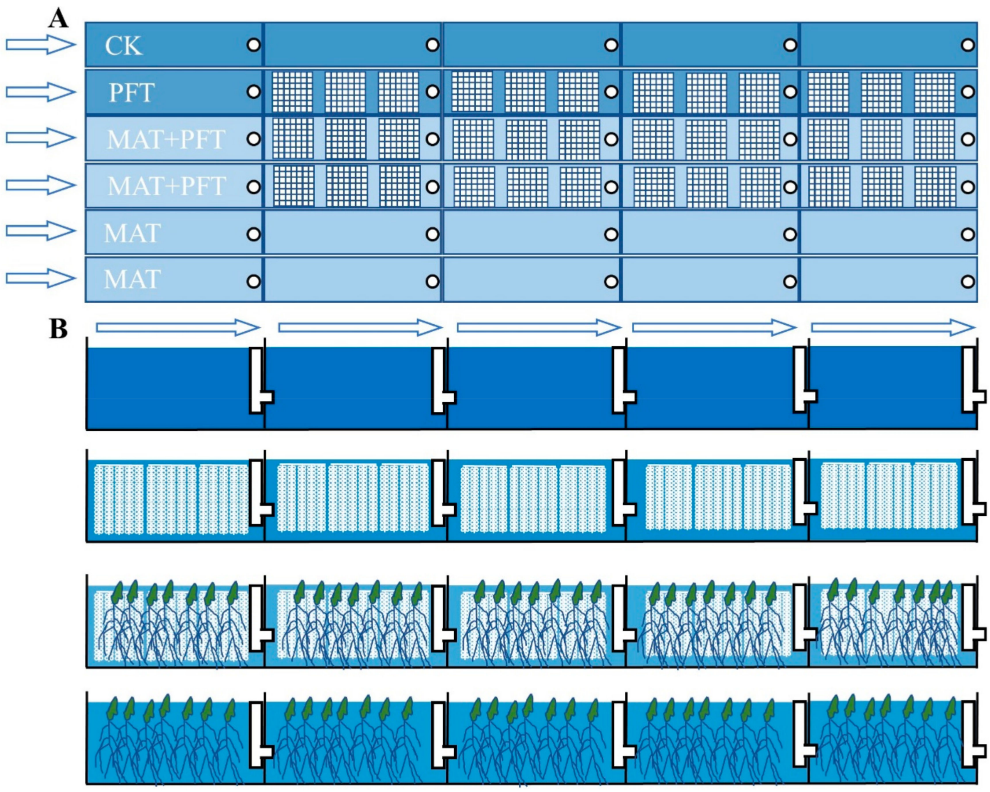

Figure 2. Schematic diagrams of the pilot-scale surface flow constructed wetlands (PSCW). Planform (**A**) and lateral views (**B**) of the PSCW are demonstrated, and the arrow points in the flow direction in the PSCWs. The treatments shown in (**A**), as control (CK), polyethylene fiber treatment (PFT), *M. aquaticum* and polyethylene fiber treatment (MAT+PFT), and *M. aquaticum* treatment (MAT), respectively, from top to bottom, are also shown in (**B**). Water-level connecting pipes controlling the water flow in the PSCW are demonstrated in each treatment stage.

Four treatments were used in the PSCW, including treatment without plants or PFs (control, CK), treatment with PFs (PFT), with *M. aquaticum* (MAT), and with *M. aquaticum* plus PFs (MAT+PFT). Similarly, *M. aquaticum* specimens were cultivated until the stem length reached 30 cm, and then transplanted into the corresponding treatments with a density of 100 plants/m^2. In order to enhance the functions of the microbial community, simplified floating beds (FBs, 2.0 m $\times$ 2.0 m) were specifically welded with 7 $\times$ 7 evenly distributed welding grids using reinforced steel bars (0.3 cm in diameter) (Figure 2A, shown in PFT and MAT+PAT treatment units). The PFs (0.7 m) were attached at every welding point under these FBs to enhance the microbial attachment. In each subunit of the PFT and MAT+PFT, three FBs with 49 PFs suspended were evenly placed with the PFs completely submerged (Figure 2B). Through long-term operation, a mature microbial community would successfully develop on the PFs; therefore, it was not necessary to perform a coating procedure on these PFs.

The HRT for the PSCW was calibrated based on the LSCW results and was set at 12.5 d for each treatment channel, making 2.5 d HRT for each subunit. The remaining parameters, including temperature, humidity, sunlight, etc., were subject to the surrounding factors as the PSCW was constructed in an open field. This experiment was conducted from February 2017 to January 2018, covering four distinct seasons of the year. The water temperature ranged from 15.2 to 34.1 °C during the experimental period.

2.6. Modelling of the PSCW and Accuracy Testing of the Models

The treatment effects of the PSCW were also investigated through the Monod models. The effluent concentrations of the PSCW were first predicted using the LSCW equations. The accuracy of these equations in predicting PSCW effluents was found by analyzing the statistical difference between the theoretical prediction and the actual performance of the PSCW. A statistical significance indicated an inaccuracy of the LSCW equations for the PSCW, and a new set of equations for the PSCW was thereafter established using the actual influent and effluent concentrations of the PSCW. The accuracy of the PSCW equations was also tested as the LSCW equations were.

2.7. Preparation of Synthetic Wastewater for the LSCW and the PSCW

Synthetic wastewater was used for the LSCW and PSCW experiment. For the LSCW, the synthetic wastewater was prepared using tap water with a final concentration (theoretical calculation) of 50 mg/L COD (glucose, Analytical Reagent, AR), 5 mg/L NH_4^+ (ammonium sulfate, AR), and 1.0 mg/L TP (monopotassium phosphate). For the daily wastewater input of the PSCW, river water (COD 12.04 mg/L, NH_4^+ 0.24 mg/L, TN 2.43 mg/L, and TP 0.05 mg/L, mean values) adjacent to the PSCW was used to prepare synthetic wastewater with a final concentration of COD 50–60 mg/L, NH_4^+ 5–8 mg/L, and TP 0.8–1.0 mg/L. Based on the designed influent concentrations, background concentrations of the river water, and daily volume of wastewater input, the amounts of reagents could be calculated (not shown in this study). For the PSCW, COD was prepared from hydroxypropyl methyl cellulose (HPMC) and cane sugar (5:1, *w*/*w*) to simulate organic matter of types both difficult and easy to biodegrade. NH_4^+ was prepared with common urea fertilizer used for local agricultural production, and TP was prepared using monopotassium phosphate and dipotassium phosphate (AR). A concentrated solution completely dissolving these reagents was first prepared (approximately 5 m^3) and then diluted with river water in a concrete pool (approximately 78 m^3) to 70 m^3. Three submerged pumps (7.5 kW, 380 V, φ100 mm outlet) were used to evenly mix the dilutions in the pool.

2.8. Water Sampling and Quality Analysis

For the LSCW, water samples were collected at 20 cm below the surface every two days for examination at the inlet, outlet, up-, and down-stream quadrants of the treatment zone. For the PSCW, water samples were collected from the inlets of every treatment and from every opening of the water-level connecting pipes. Water qualities including COD, NH_4^+, TN, and TP were examined through well-established standard methods published in previous studies [38,42], unless otherwise specified.

2.9. Routine Maintenance of the LSCW and the PSCW

An important aspect of both the LSCW and the PSCW is routine maintenance, which mainly includes cleaning the debris of macrophytes and harvesting overgrown plant tissues. For the LSCW, routine maintenance was performed every two weeks; for the PSCW, routine maintenance was conducted every 40 days during the local winter and spring (November to April of the next year) and every two weeks during the local summer and autumn (April to October). The debris and overgrown plant tissues were cut and harvested manually, leaving the healthy plants for the experiment.

3. Data and Statistical Analyses

The pollutant removal efficiencies of the LSCW were calculated using the difference between the influent and effluent divided by the influent concentration (mg/L). Similarly, the removal efficiencies at the end of each treatment stage of the PSCW were calculated using the difference of pollutant concentrations (mg/L) between the initial influent and the stage effluent divided by the initial influent concentration (mg/L). The calculation for the organic loading rates of the pollutants was adopted from a previous study [42]. One-way univariate analysis of variance (ANOVA) was used to analyze the statistical significance of removal efficiencies of different treatments in the LSCW and the PSCW. Paired-sample *t*-testing was used to observe the statistical significance between two treatments (such as PFT and MAT), as well as the statistical significance between theoretical predictions and actual performance when testing the model accuracy. All the statistical analyses were performed using GraphPad Software (v7.0, Inc., San Diego, CA, USA), and the collective significant level was at 0.01.

4. Results and Discussion

4.1. HRTs Affect the Pollutant Removal Efficiencies in the LSCW

HRT is one of the most essential factors affecting the nutrient removal efficiencies of CWs [11,15]. Herein, the effects of 4 d and 7 d on the removal of COD, NH_4^+, TN, and TP by different treatments (MAT, ECT, and PFT) were studied. In general, the LSCW showed better removal efficiencies at 7 d compared with removal efficiencies at 4 d (Figures 3 and 4). At 7 d HRT, the LSCW achieved COD removal efficiencies at 68.8%, 52.7%, and 38.9% with treatments of *M. aquaticum*, *E. crassipes*, and PFs with influent COD concentrations of 53.16, 52.65, and 57.71 mg/L, respectively (Figure 3B). NH_4^+ was reduced by 82.1%, 66.4%, and 35.8% through the same treatments with influent NH_4^+ concentrations of 5.06, 5.00, and 4.97 mg/L, respectively (Figure 3D). The LSCW also achieved relatively high removal efficiencies on TN through *M. aquaticum* treatment (50.0%) with influent TN at 10.59 mg/L, whilst treatments of the LSCW with *E. crassipes* and PFs did not show much TN reduction (Figure 4B). TP removal efficiencies by the LSCW reached 66.1%, 41.7%, and 16.3% with influent TP concentrations of 1.01, 0.99, and 0.97 mg/L, respectively (Figure 4D).

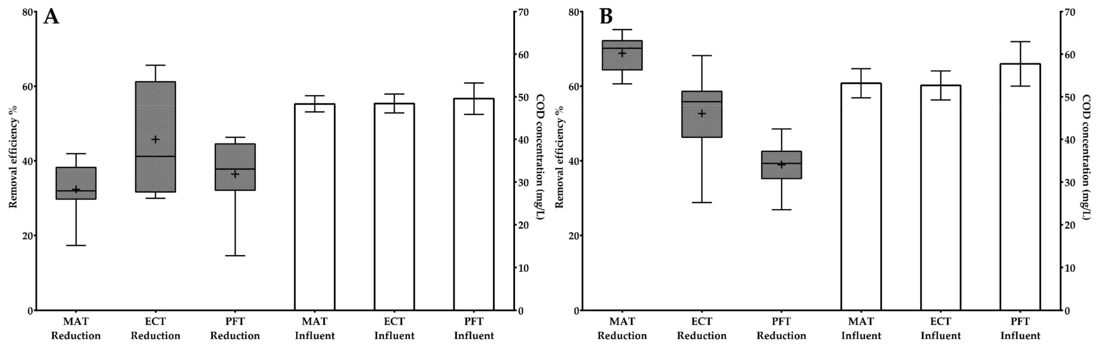

Figure 3. *Cont.*

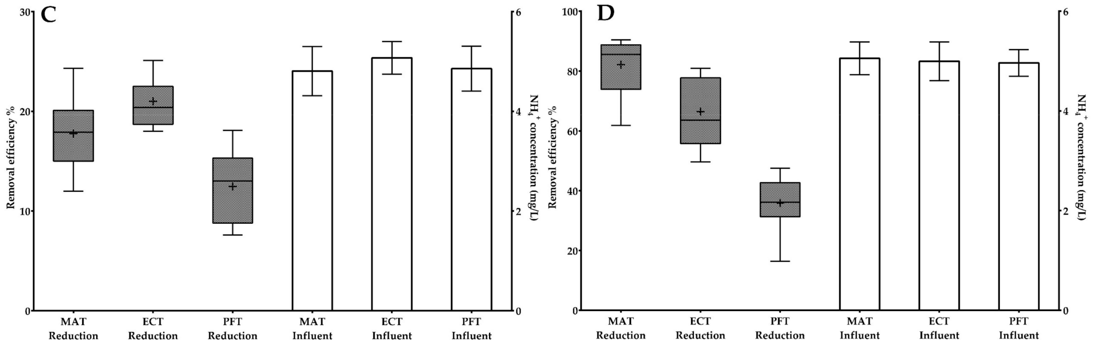

Figure 3. Removal efficiencies and influents of chemical oxygen demand (COD) and NH_4^+ in the LSCW at different hydraulic retention times (HRTs). COD influents and removal efficiencies by different treatments are shown at HRTs of 4 d (**A**) and 7 d (**B**), whilst NH_4^+ influents and removal efficiencies are shown at 4 d (**C**) and 7 d (**D**). MAT, ECT, and PFT represent LSCW treatment with *M. aquaticum*, *E. crassipes*, and polyethylene fiber, respectively. Black solid lines and plus signs represent the median and mean of the datasets, respectively. The bottom and top edges of the box plots indicate the 25th and 75th percentiles, and the whiskers illustrate the 2.5th and 97.5th percentiles. The bar plots stand for the means of influent pollutant concentrations, and error bars for the standard deviation (SD).

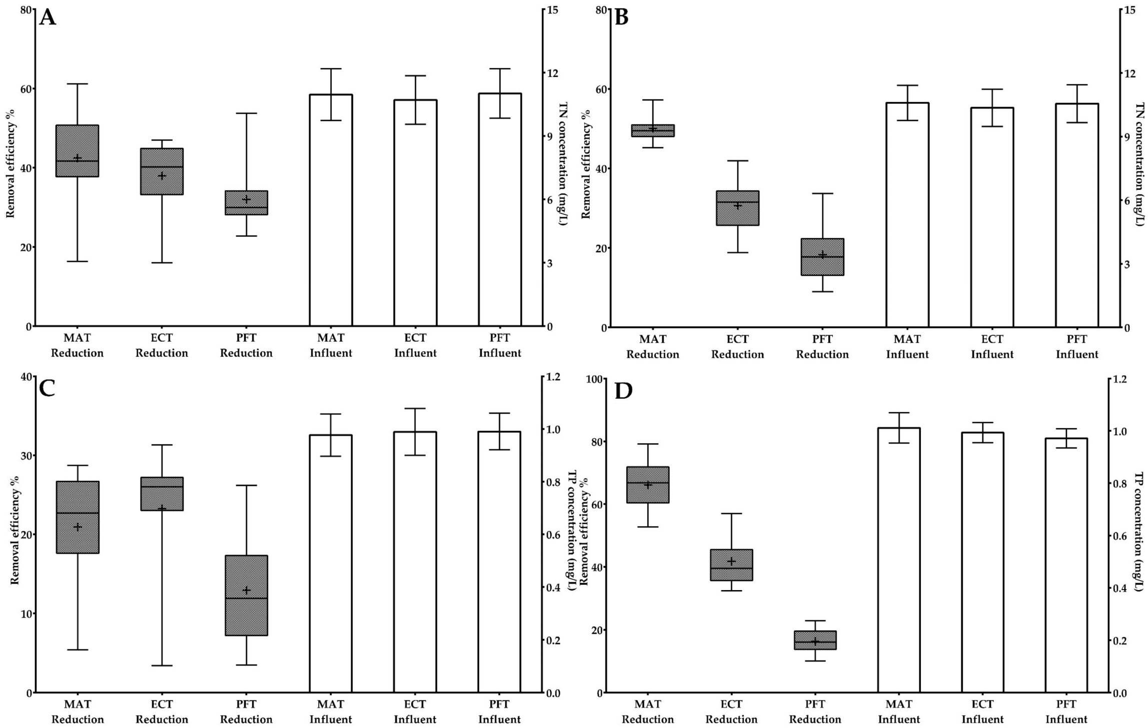

Figure 4. Removal efficiencies and influents of total nitrogen (TN) and total phosphorus (TP) in the LSCW at different HRTs. TN influents and removal efficiencies for different treatments are shown at HRTs of 4 d (**A**) and 7 d (**B**), whilst TP influents and removal efficiencies are shown at 4 d (**C**) and 7 d (**D**). MAT, ECT, and PFT represent LSCW treatment with *M. aquaticum*, *E. crassipes*, and polyethylene fiber, respectively. Black solid lines and plus signs represent the median and mean of the datasets, respectively. The bottom and top edges of box plots indicate the 25th and 75th percentiles, and the whiskers illustrate the 2.5th and 97.5th percentiles. The bar plots stand for the means of influent pollutant concentrations, and error bars for the standard deviation (SD).

The shortened HRT resulted in significantly decreased ($p < 0.01$) removal efficiencies for all the pollutants by all the treatments (MAT, ECT, and PFT). The alteration of HRT from 7 d (0.56 m^3/d) to 4 d (0.98 m^3/d) caused a quicker flow through the treatment zones in the LSCW, which greatly reduced the contact time with the filling substrates (macrophytes or PFs). The prolonged HRT may also facilitate the establishment of an appropriate microbial community on the PFs and root surfaces of macrophytes, which enables adequate time to contact with and remove pollutants [49]. These observations were consistent with those of previous studies, which reported the significantly increased removal of NH_4^+ and TN in treated effluent with the increase of HRT in CWs treating domestic wastewater [50,51].

However, further prolonged HRT in this LSCW may reverse the effects: a 14 d treatment period was conducted, and this prolongation rendered a dramatic reduction in water flow and resulted in greatly decreased removal efficiencies (data not shown). This may be due to the overgrowth of macrophytes, which lowered the dissolved oxygen content in the water and decelerated the microbial activity on pollutant removal [52]. The overgrowth of macrophytes also quickened the apoptosis of plants, and decomposition of fallen-off plant debris may return the assimilated and absorbed nutrients back to the water and accelerate the deterioration of water quality (data not shown). Therefore, the optimal HRT was 7 d for the LSCW.

4.2. Macrophytes Showed Excellent Nutrient Removal in the LSCW

Macrophytes played an essential role in the removal of nutrients, especially the eutrophic N and P pollutants, and the efficiencies may vary between different plant species, as was shown in the LSCW. For the 7 d treatment experiment, the CW planted with *M. aquaticum* showed significantly higher ($p < 0.01$) removal efficiencies on NH_4^+ and TP compared with that planted with *E. crassipes* (Figures 3 and 4). Besides NH_4^+ and TP removal, the CW with *M. aquaticum* also exhibited significantly higher ($p < 0.01$) removal capabilities on COD and TN than that with *E. crassipes* did (Figures 3 and 4). The results collectively indicated that *M. aquaticum* planted in the LSCW was a better macrophyte for removing these pollutants from wastewater. The mechanism of pollutant removal may be attributed to plant uptake for growth and proliferation as reported in other studies [27,42,53]. For instance, mass balance analyses in these studies showed that *M. aquaticum* can uptake 1.06–1.44 g N and 1.02–1.67 g P/kg dry weight, which is generally higher than the N and P uptake rates by macrophytes such as *Phragmites australis* and *Typha orientalis*. The highly effective removal capability may also correlate with the activities of various functional microbial communities, as *M. aquaticum* might create an aerobic micro-environment by secreting oxygen through submerged plant tissues to facilitate microbial metabolic activities [52,54]. It was reported that *M. aquaticum* in CWs treating swine wastewater could shift the functional microbial community, upregulating expression of functional genes responsible for complete nitrification and denitrification to facilitate NH_4^+ and TN removal [38]. Considering its superior capability for removing eutrophic N and P nutrients and its characteristic of enhancing microbial activities, *M. aquaticum* was selected in the subsequent PSCW experiment.

4.3. COD and NH_4^+ Removal in the LSCW Complied with Models

A Monod kinetic model was used to describe and evaluate the pollutant removal dynamics in the LSCW. The hydraulic inflow pattern in this LSCW was thought to be similar to that of the plug flow pattern [46]. Therefore, model equations of COD and NH_4^+ removal in the LSCW were established by correlating the Monod models with the plug flow dynamic pattern (general Equation (1)). During the experimental period (4 d and 7 d HRT collectively), the mean influent COD and NH_4^+ concentrations were 51.72 mg/L and 4.98 mg/L, and the mean effluent COD and NH_4^+ were 21.25 mg/L and 1.72 mg/L, respectively (Table 1). Each influent/effluent concentration (C_{in} and C_{out}) with corresponding daily water influent (Q) and treatment area of the LSCW (A_h, 16 m × 0.5 m, L × W) was used to calculate the *K* values (rate constants). The geometric means of the *K* values of COD and NH_4^+ were taken to establish the model equations as follows:

$$C_{COD\ in} - C_{COD\ out} + 60 \times \ln\left(\frac{C_{COD\ in}}{C_{COD\ out}}\right) = 6.62 \times \frac{A_{h\ LSCW}}{Q_{\ LSCW}} \quad (3)$$

$$C_{NH_4^+\ in} - C_{NH_4^+\ out} + 0.05 \times \ln\left(\frac{C_{NH_4^+\ in}}{C_{NH_4^+\ out}}\right) = 0.227 \times \frac{A_{h\ \mathrm{LSCW}}}{Q_{\ \mathrm{LSCW}}} \tag{4}$$

The accuracy of these models was tested using the established Equations (3) and (4) to calculate the theoretical effluent COD and NH_4^+ concentrations, respectively. In comparison, no statistical significance ($p > 0.01$) was determined between the theoretical calculation and the actual effluents (Figure S1A). Therefore, the established equations were accurate in reflecting and predicting the pollutant concentrations of the LSCW effluent.

Table 1. Influent, effluent, and *K* values of COD and NH_4^+ for LSCW modelling.

Parameters	Numbers of Values	Minimum	Median	Maximum	Mean (M) or Geometric Mean (GM)	Standard Deviation (SD) or Geometric SD (GSD)
COD influent (mg/L)	26	45.24	51.50	61.07	51.72 (M)	3.73 (SD)
COD effluent (mg/L)	26	13.47	17.59	35.05	21.25 (M)	7.62 (SD)
NH_4^+ influent (mg/L)	26	4.07	5.01	5.6	4.98 (M)	0.39 (SD)
NH_4^+ effluent (mg/L)	26	0.49	1.26	4.40	1.72 (M)	1.41 (SD)
K_{COD} ($g{\cdot}m^{-2}{\cdot}d^{-1}$)	26	4.179	6.7	8.797	6.62 (GM)	1.25 (GSD)
K_{NH4^+} ($g{\cdot}m^{-2}{\cdot}d^{-1}$)	26	0.104	0.285	0.36	0.227 (GM)	1.56 (GSD)

4.4. The PSCW Designed from the LSCW

The PSCW was designed to increase the daily input to 10 times that of the LSCW. The LSCW demonstrated best removal efficiencies at an input of 0.56 m^3/d at 7 d HRT; therefore, the input for the PSCW was chosen to be 5.6 m^3/d at least. With the designed influent concentrations (COD 50 mg/L and NH_4^+ 5 mg/L), expected effluent concentrations (COD 30 mg/L and NH_4^+ 1.5 mg/L), and the daily input set, the required A_h for the PSCW was calculated through Equations (3) and (4). A greater surface area is required for NH_4^+ treatment: 87.83 m^2 against the 42.85 m^2 required for COD treatment.

Previous studies have demonstrated that a multistage treatment strategy could further enhance the treatment efficiency of CWs [42,48]; therefore, the design of the PSCW also adopted this strategy. Based on the related CW frame structure [42], integrating the requirement of treatment area for pollutant removal and local land usage, the PSCW was finally designed as a pondlike system consisting of six parallel treatment units (Figure 2A), each of which was 80 m^2 (40 m $\times$ 2.0 m) with a depth of 1.0 m. Each treatment unit was evenly divided into five subunits to simulate the previous system [42].

4.5. The PSCW Showed Enhanced Removal of NH_4^+ and TN

Synthetic wastewaters containing an average NH_4^+ concentration of 8.78–9.02 mg/L were pumped into each treatment of the PSCW (Figures 2 and 5A). The first stage of all four treatments showed considerable NH_4^+ reduction: 39% of NH_4^+ was removed in the first stage of CK, 46.2% in PFT, 50.8% in MAT, and 52.7% in MAT with PFs. After the third stage, the NH_4^+ contents were overall reduced by 66.9% in CK, 79.3% in PFT, 82.9% in MAT, and 84.4% in MAT with PFs. In the effluents, the NH_4^+ contents were finally reduced 80.8%, 86.0%, 95.7%, and 96% in CK, PFT, MAT, and MAT with PFs, respectively (Figure 5B). The influent contained TN at a concentration of 10.62–10.75 mg/L (Figure 5C), and the first stages of CK, PFT, MAT, and MAT with PFs removed 25.6%, 28%, 38.2%, and 36.8% of this TN, respectively. After the third stage, the TN reduction reached 58.0% in CK, 52.7% in PFs, 69.3% in MAT, and 70.1% in MAT with PFs. The final TN removal efficiencies reached 71.8% in CK, 67.6% in PFs, 78.6% in MAT, and 80.2% in MAT with PFs (Figure 5D).

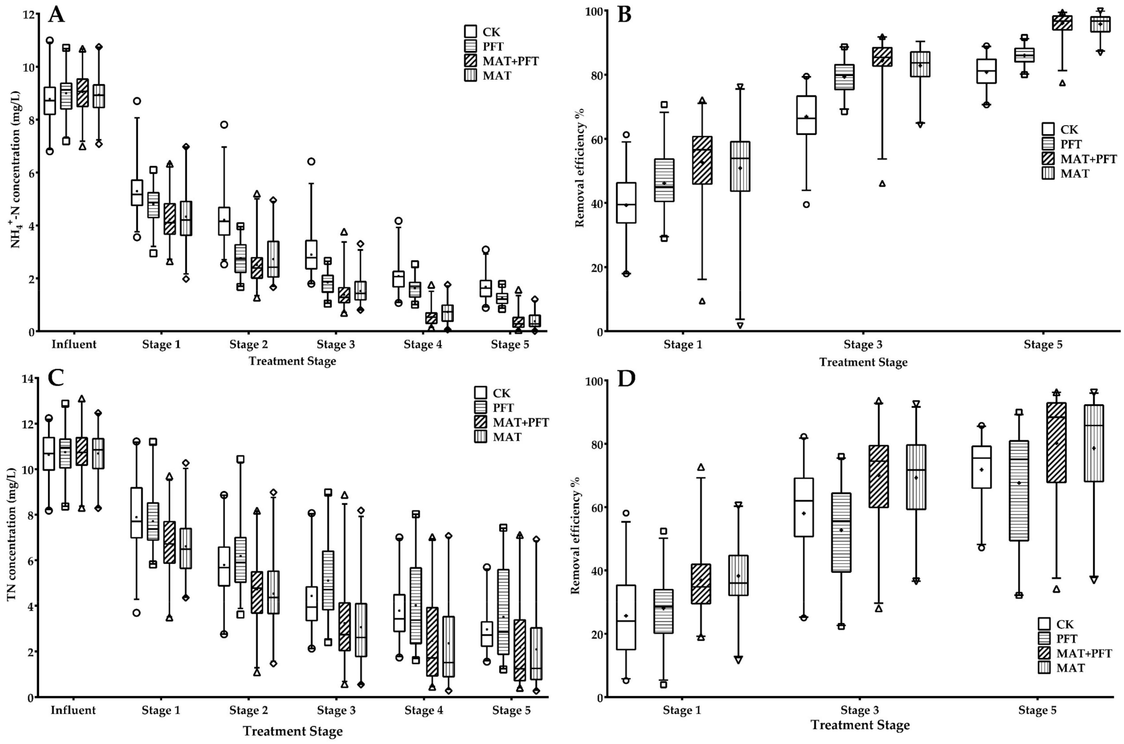

Figure 5. Changes of NH_4^+ (**A**) and TN concentrations (**C**) as well as removal efficiencies of NH_4^+ (**B**) and TN (**D**) in the PSCW. CK, PFT, MAT, and MAT with PFT represent the control and PSCW treatments with polyethylene fiber, *M. aquaticum*, and *M. aquaticum* with polyethylene fiber, respectively. Black solid lines and plus signs represent the median and mean of the datasets, respectively. The bottom and top edges of the box plots indicate the 25th and 75th percentiles, and the whiskers illustrate the 2.5th and 97.5th percentiles.

The CK also showed NH_4^+ and TN removal during the experiment period, which indicated that without any external treatments (*M. aquaticum* or an enhanced microbial community on PFs), the in situ microbial community could also reduce NH_4^+ and remove the TN to some extent. However, even though the removal efficiency was considerable, the relatively high concentration of NH_4^+ and TN in the CK effluents (Figure 5A, 1.68 $\pm$ 0.44 and 2.97 $\pm$ 1.06 mg/L, respectively) may still place risks on the aquatic environment [4,7]. The introduction of PFs enhanced the attachment of functional microbial communities, which significantly reduced the NH_4^+ concentration (1.25 mg/L, $p < 0.01$) in the effluents, indicating that the NH_4^+ oxidizing community might be enriched through PFs [39,43].

Compared with CK, MAT showed significantly ($p < 0.01$) strengthened removal of NH_4^+ and TN (95.7% and 78.6%, respectively, Figure 5B,D), as also shown in the LSCW. Additionally, compared with MAT, MAT with PFs significantly increased ($p < 0.01$) the removal efficiencies of corresponding pollutants, which indicated that MAT with PFs in the PSCW was most effective for eutrophic N removal.

Due to the low treatment level of most wastewater treatment plants in China, the relatively high concentration of eutrophic N in the effluents may exceed the capacity of the receiving aquatic environments [8,9]. In this study, floating bed technology was supplemented with *M. aquaticum* in the PSCW, which showed excellent removal capabilities on a relatively high concentration of NH_4^+ (8.78–9.02 mg/L) and TN (10.62–10.75 mg/L). The final removal efficiency of NH_4^+ reached a maximum at 95.7%, higher than the reported removal efficiencies of 40–75% in other CWs [55–57]. The final removal efficiency of TN amounted to 78.6%, which was also higher than that reported in previous studies [58,59]. The functional microbial community may also contribute to NH_4^+ and TN removal, and *M. aquaticum* can dramatically strengthen these communities for nitrogen cycling, as reported in previous studies [27,38].

4.6. Removal of COD and Relationship Between COD and N Removal in the PSCW

HPMC with supplementary cane sugar was used to represent the main components of COD in the PSCW. The mean COD concentrations in the influents were 56.5–57.5 mg/L (Figure 6A). HPMC is relatively difficult to biodegrade; therefore, the removal efficiencies in the first stage were 5.8%, 14.6%, 23.4%, and 25.9% in CK, PFT, MAT, and MAT with PFT, respectively (Figure 6B). In the effluents of each PSCW treatment, the COD concentration dropped to 39.9, 33.4, 27.0, and 24.6 mg/L in CK, PFT, MAT, and MAT with PFT, rendering final removal efficiencies of 29.6%, 41.5%, 52.3%, and 56%, respectively. In comparison with CK, the treatment approaches (PFT, MAT, and MAT with PFT) significantly enhanced ($P < 0.01$) the COD removal.

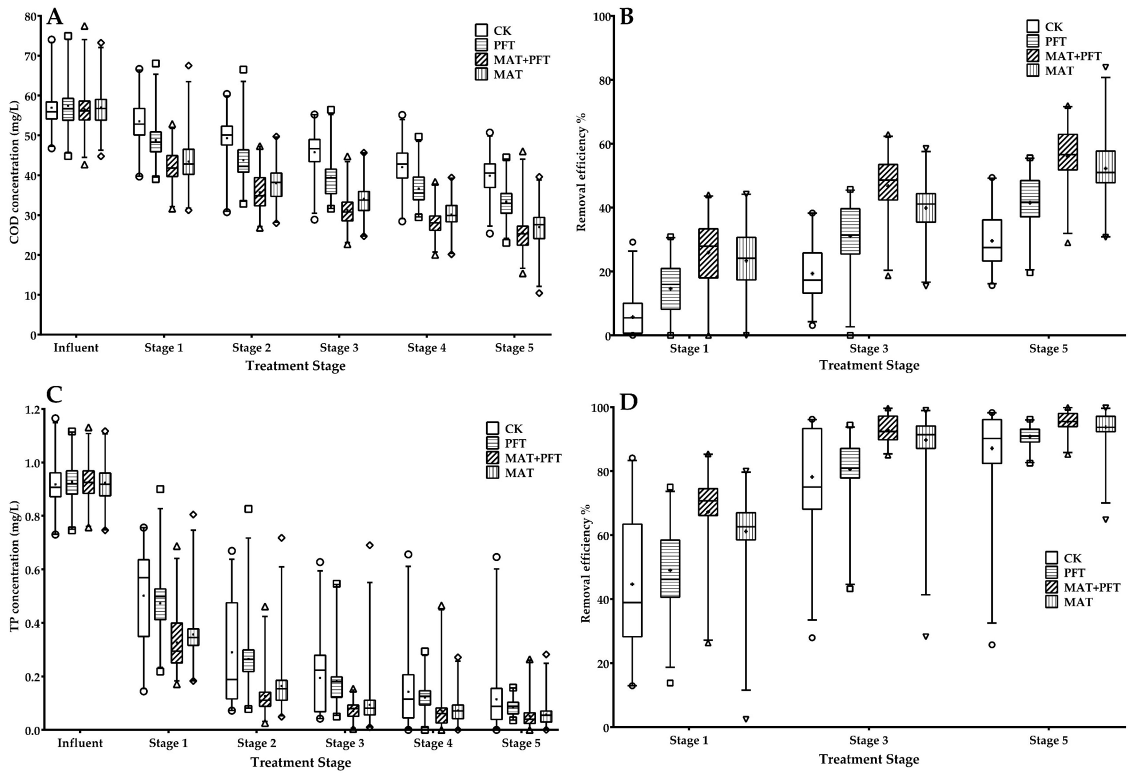

Figure 6. Changes of COD (**A**) and TP concentrations (**C**), as well as removal efficiencies of COD (**B**) and TP (**D**) in the PSCW. CK, PFT, MAT, and MAT with PFT represent the control and PSCW treatments with polyethylene fiber, *M. aquaticum*, and *M. aquaticum* with polyethylene fiber, respectively. Black solid lines and plus signs represent the median and mean of the datasets, respectively. The bottom and top edges of the box plots indicate the 25th and 75th percentiles, and the whiskers illustrate the 2.5th and 97.5th percentiles.

Similar to the wastewater treatment process, carbon sources are also essential in the CWs' treatment of nutritional N [60–62]. Glucose would have been used as the main carbon source in the PSCW; however, the glucose was considerably easily biodegradable, which may stimulate the growth of the microbial community in the initial stage but fail the communities in subsequent treatment stages (data not shown). Therefore, in order to complement COD and sustain the carbon supply, cane sugar was supplemented with HPMC (1:5, *w*/*w*). Based on the N removal dynamics, the addition of HPMC may support enhanced N removal along the PSCW treatment channels. A previous study using a subsurface flow CW to treat wastewater demonstrated that a COD/N ratio of 5 was most effective in the removal of N and COD from the synthetic wastewater [60,62]. Under such a COD/N ratio, the best TN and COD removal efficiencies achieved were over 80% and 90% in the CWs planted with *Phragmites australis*; however, NH_4^+ removal was significantly decreased. In contrast, in an integrated vertical flow CW, the increase of the COD/N ratio promoted the removal of NH_4^+ (90%) and TN

(55–90%) [63]. For this PSCW, the COD/N ratio in the influent was 5–6, and during the experimental period, the best removal efficiencies of NH_4^+ and TN reached 96% and 80.2%, respectively. The results indicated that, under current operational conditions, a combination of HPMC and cane sugar as the carbon source could dramatically enhance the N removal; the actual mechanism behind this will be investigated in future work.

4.7. The PSCW Showed Excellent TP Removal Capability and Potential

The TP concentration for the PSCW treatments was 0.92–0.93 mg/L on average (Figure 6C). Similar with the reduction of N, TP was considerably removed in the first stage of the four treatments (Figure 6D). After the treatment in the third stage, the TP concentration significantly decreased ($p < 0.01$) to 0.19, 0.18, 0.09, and 0.07 mg/L in CK, PFT, MAT, and MAT with PFT, respectively, giving removal efficiencies of 78.2%, 80.6%, 89.7%, and 92.8%. In the effluents of each treatment, the TP contents were finally reduced by 87.1%, 90.8%, 93.7%, and 95.4% in CK, PFT, MAT, and MAT with PFT, respectively (Figure 6D).

It has been broadly acknowledged that the main mechanisms for P removal in CWs are plant and microbial uptake for growth, substrate adsorption, and precipitation to the sediment [32,42,64]. In the PSCW, treatments with *M. aquaticum* (MAT and MAT with PFs) achieved considerably high efficiency in TP removal, which indicated that *M. aquaticum* played a more important role in TP removal than did the enhanced microbial community. In comparison between CK and PFT, it can be seen that the enhanced microbial community could increase the TP removal but with limited capacity. Additionally, compared with the influent TP concentrations, the relatively high removal efficiency in CK and PFT inferred that TP removal may also be attributed to a precipitation process. However, physical mechanisms such as precipitation and sorption could not sustain substantial TP removal for long-term operation, as the substrates and adsorption materials could become saturated, losing the capacity for TP sequestration. It was observed that the CWs operated for a short period could remove over 90% of TP; however, the removal efficiencies decreased significantly after a prolonged operation period even at lower TP inputs [65,66]. Moreover, the PSCW grown with *M. aquaticum* exhibited greater capacity potential for TP removal: after the third-stage treatment of the PSCW, TP was already considerably reduced, leaving the remaining two treatment units not fully exploited (Figure 6C,D). Therefore, this composite CW showed great potential in treating wastewater with a high concentration of P, as indicated in a previous study [42].

4.8. COD and NH_4^+ Removal in the PSCW Complied with Models

The accuracy of model equations established for the LSCW was examined in terms of predicting the PSCW performance. For the convenience of operation and preparation of influent water, the HRT for each PSCW treatment (80 m^3) was calibrated to 12.5 d, which makes the influent 6.4 m^3/d. With the determined influent COD and NH_4^+, surface area, and daily influent volume, the effluent COD and NH_4^+ were calculated through Equations (3) and (4), respectively. The theoretical calculations were compared with the actual performance of the PSCW, and statistical significances ($p < 0.01$) were observed (Figure S1B); these indicated that the equations for the LSCW were not applicable to simulating the effluent COD and NH_4^+ in the PSCW.

The theoretical effluent of COD was significantly ($p < 0.01$) lower than that of the actual effluent. The significance was mainly due to the different nature of the carbon source used in these two CW systems: glucose was the sole carbon source in the LSCW, whilst HPMC with supplementary cane sugar was used in the PSCW [67]. Therefore, the rate constant will be different due to different degradation dynamics on altered carbon sources. Additionally, the increased hydraulic daily input (6.4 m^3/d compared with the designed 5.6 m^3/d), which reduced the HRT, would also affect the degradation of carbon sources [68].

On the contrary, the theoretical effluent of NH_4^+ was significantly ($p < 0.01$) higher than that of the actual effluent, which demonstrated that the enlarged PSCW from the LSCW significantly enhanced the removal of NH_4^+. This significant difference can be attributed to the more active physiochemical reactions, such as oxygen exchange at the air–water interface, plant uptake, and microbial degradation, etc., that occurred in PSCW compared with in the LSCW; these greatly favored the transformation of NH_4^+ into other forms of nitrogen. The mechanisms behind this will be investigated in detail in future studies.

Therefore, new model equations for the PSCW complying with the general Monod models (Equation (1)) were developed using the corresponding parameters (Table 2). Similarly, the geometric means of the K values were taken to establish the model equations as follows:

$$C_{COD\ in} - C_{COD\ out} + 60 \times \ln\left(\frac{C_{COD\ in}}{C_{COD\ out}}\right) = 5.866 \times \frac{A_{h\ PSCW}}{Q_{PSCW}} \quad (5)$$

$$C_{NH_4^+\ in} - C_{NH_4^+\ out} + 0.05 \times \ln\left(\frac{C_{NH_4^+\ in}}{C_{NH_4^+\ out}}\right) = 0.696 \times \frac{A_{h\ PSCW}}{Q_{PSCW}} \quad (6)$$

The accuracy of these models was tested in the same way as the LSCW equations were. The theoretical effluent COD and NH_4^+ concentrations of the PSCW were compared with the actual effluent concentrations, and no statistical significance ($p > 0.01$) was determined (Figure S1C). Therefore, the established equations were accurate for reflecting and predicting the effluent concentrations of the PSCW.

Table 2. Influent, effluent, and K values of COD and NH_4^+ for PSCW modelling.

Parameters	Numbers of Values	Minimum	Median	Maximum	Mean (M) or Geometric Mean (GM)	Standard Deviation (SD) or Geometric SD (GSD)
COD influent (mg/L)	50	44.75	56.74	73.24	56.97 (M)	4.83 (SD)
COD effluent (mg/L)	50	10.42	27.6	39.59	26.99 (M)	4.87 (SD)
NH_4^+ influent (mg/L)	50	7.08	8.92	10.75	8.94 (M)	0.76 (SD)
NH_4^+ effluent (mg/L)	50	0.011	0.28	1.21	0.38 (M)	0.28 (SD)
K_{COD} ($g \cdot m^{-2} \cdot d^{-1}$)	50	3.15	5.73	13.1	5.866 (GM)	1.286 (GSD)
K_{NH4^+} ($g \cdot m^{-2} \cdot d^{-1}$)	50	0.56	0.70	0.88	0.696 (GM)	1.099 (GSD)

5. Conclusions

This study evaluated the capability of a LSCW and a PSCW in terms of the removal of COD, NH_4^+, TN, and TP from synthetic wastewater. In the LSCW, reduced HRT (7 d to 4 d) led to significantly reduced removal efficiencies for each pollutant, and the HRT was optimized at 7 d accordingly. Based on the optimized parameters, Monod models combined with plug flow pattern dynamics were established for the LSCW and were used to guide the enlarged design of the PSCW. The up-scaled PSCW planted with *M. aquaticum* and polyethylene fibers exhibited significantly enhanced capability for removing these pollutants compared with the LSCW treatments, especially the N and P pollutants such as NH_4^+, TN, and TP. The PSCW's performance greatly exceeded its predicted treatment capability, indicating the great application potential of such a CW system for the advanced treatment of wastewater effluents. In general, the up-scaled design from the LSCW and the operation of this PSCW were successful. Both the LSCW and the PSCW planted with *M. aquaticum* exhibited excellent properties of eutrophic N and P removal from the polluted waters, which makes this macrophyte appropriately applicable in constructed wetland systems. The mechanisms behind pollutant removal in these tested CW systems may mainly be uptake by macrophytes and microbial communities, precipitation to sediments, and substrate adsorption. Therefore, mass balance analyses on these pollutants are needed to figure out the key mechanisms in future work.

Supplementary Materials: The following are available online at http://www.mdpi.com/2073-4441/10/10/1391/s1, Figure S1: Comparison of theoretical and actual concentrations of COD and NH_4^+ in the LSCW and the PSCW. Theoretical concentrations of COD and NH_4^+ were predicted through the established Monod model equations for the LSCW and the PSCW. (A) shows the accuracy test of the LSCW model equations for representing the LSCW performance; (B) shows the significant difference between the theoretical prediction of the PSCW performance using the LSCW equations and the actual performance of the PSCW; (C) shows the accuracy test of the PSCW model equations for representing the PSCW performance. Paired *t*-testing was performed, and the statistical significance is presented as follows: * $p < 0.05$, ** $p < 0.01$, *** $p < 0.001$, and **** $p < 0.0001$.

Author Contributions: S.F., X.Z., R.W. and X.M. conceived of and performed the experiments, and wrote the paper. X.Z., G.Z., Z.B., S.X. and Z.Z. contributed to the discussion and analyzed the experiments.

Funding: This research was supported by the National Water Pollution Control and Treatment Science and Technology Major Project (2015ZX07206006), the Innovation in Cross-Functional Team Program of the Chinese Academy of Sciences (No. 2015), the Key Research Program of Chinese Academy of Sciences (ZDRW-ZS-2016-5), and the Key Research and Development Project of Hebei Province (18273615D).

Acknowledgments: Special thanks to Weidong Zhang, who substantially contributed to routine maintenance of the constructed wetlands.

Conflicts of Interest: The authors declare no competing financial interests.

References

1. Li-kun, Y.; Sen, P.; Xin-hua, Z.; Xia, L. Development of a two-dimensional eutrophication model in an urban lake (China) and the application of uncertainty analysis. *Ecol. Model.* **2017**, *345*, 63–74. [CrossRef]
2. Smith, V.H.; Schindler, D.W. Eutrophication science: Where do we go from here? *Trends Ecol. Evol.* **2009**, *24*, 201–207. [CrossRef] [PubMed]
3. Chloupek, O.; Hrstkova, P.; Schweigert, P. Yield and its stability, crop diversity, adaptability and response to climate change, weather and fertilisation over 75 years in the Czech Republic in comparison to some European countries. *Field Crop Res.* **2004**, *85*, 167–190. [CrossRef]
4. Carpenter, S.R.; Caraco, N.F.; Correll, D.L.; Howarth, R.W.; Sharpley, A.N.; Smith, V.H. Nonpoint pollution of surface waters with phosphorus and nitrogen. *Ecol. Appl.* **1998**, *8*, 559–568. [CrossRef]
5. Smith, V.H.; Tilman, G.D.; Nekola, J.C. Eutrophication: Impacts of excess nutrient inputs on freshwater, marine, and terrestrial ecosystems. *Environ. Pollut.* **1999**, *100*, 179–196. [CrossRef]
6. Rast, W.; Thornton, J.A. Trends in eutrophication research and control. *Hydrol. Process* **1996**, *10*, 295–313. [CrossRef]
7. Serrano, L.; Reina, M.; Quintana, X.D.; Romo, S.; Olmo, C.; Soria, J.M.; Blanco, S.; Fernandez-Alaez, C.; Fernandez-Alaez, M.; Caria, M.C.; et al. A new tool for the assessment of severe anthropogenic eutrophication in small shallow water bodies. *Ecol. Indic.* **2017**, *76*, 324–334. [CrossRef]
8. Zhang, Q.H.; Yang, W.N.; Ngo, H.H.; Guo, W.S.; Jin, P.K.; Dzakpasu, M.; Yang, S.J.; Wang, Q.; Wang, X.C.; Ao, D. Current status of urban wastewater treatment plants in China. *Environ. Int.* **2016**, *92*, 11–22. [CrossRef] [PubMed]
9. Zhang, S.N.; Xiao, R.L.; Liu, F.; Zhou, J.; Li, H.F.; Wu, J.S. Effect of vegetation on nitrogen removal and ammonia volatilization from wetland microcosms. *Ecol. Eng.* **2016**, *97*, 363–369. [CrossRef]
10. Chen, Y.; Wen, Y.; Zhou, Q.; Vymazal, J. Effects of plant biomass on denitrifying genes in subsurface-flow constructed wetlands. *Bioresour. Technol.* **2014**, *157*, 341–345. [CrossRef] [PubMed]
11. Wu, H.M.; Zhang, J.; Li, C.; Fan, J.L.; Zou, Y.N. Mass balance study on phosphorus removal in constructed wetland microcosms treating polluted river water. *Clean-Soil Air Water* **2013**, *41*, 844–850. [CrossRef]
12. Vymazal, J. Plants used in constructed wetlands with horizontal subsurface flow: A review. *Hydrobiologia* **2011**, *674*, 133–156. [CrossRef]
13. Wu, S.B.; Kuschk, P.; Brix, H.; Vymazal, J.; Dong, R.J. Development of constructed wetlands in performance intensifications for wastewater treatment: A nitrogen and organic matter targeted review. *Water Res.* **2014**, *57*, 40–55. [CrossRef] [PubMed]
14. Yalcuk, A.; Ugurlu, A. Comparison of horizontal and vertical constructed wetland systems for landfill leachate treatment. *Bioresour. Technol.* **2009**, *100*, 2521–2526. [CrossRef] [PubMed]
15. Badhe, N.; Saha, S.; Biswas, R.; Nandy, T. Role of algal biofilm in improving the performance of free surface, up-flow constructed wetland. *Bioresour. Technol.* **2014**, *169*, 596–604. [CrossRef] [PubMed]

16. Harrington, C.; Scholz, M. Assessment of pre-digested piggery wastewater treatment operations with surface flow integrated constructed wetland systems. *Bioresour. Technol.* **2010**, *101*, 7713–7723. [CrossRef] [PubMed]
17. Saeed, T.; Sun, G.Z. A review on nitrogen and organics removal mechanisms in subsurface flow constructed wetlands: Dependency on environmental parameters, operating conditions and supporting media. *J. Environ. Manag.* **2012**, *112*, 429–448. [CrossRef] [PubMed]
18. Cui, L.H.; Ouyang, Y.; Lou, Q.A.; Yang, F.L.; Chen, Y.; Zhu, W.L.; Luo, S.M. Removal of nutrients from wastewater with *Canna indica* L. under different vertical-flow constructed wetland conditions. *Ecol. Eng.* **2010**, *36*, 1083–1088.
19. Meng, P.P.; Pei, H.Y.; Hu, W.R.; Shao, Y.Y.; Li, Z. How to increase microbial degradation in constructed wetlands: Influencing factors and improvement measures. *Bioresour. Technol.* **2014**, *157*, 316–326. [CrossRef] [PubMed]
20. Koottatep, T.; Phong, V.H.N.; Chapagain, S.K.; Panuvatvanich, A.; Polprasert, C.; Ahn, K.H. Performance evaluation of selected aquatic plants and iron-rich media for removal of PPCPs from wastewater in constructed wetlands. *Desalin. Water Treat.* **2017**, *91*, 281–286. [CrossRef]
21. Surrency, D. *Evaluation of Aquatic Plants for Constructed Wetlands. Constructed Wetlands for Water Quality Improvement*; Lewis Publishers: Boca Raton, FL, USA, 1993.
22. Xu, J.T.; Zhang, J.A.; Xie, H.J.; Li, C.; Bao, N.; Zhang, C.L.; Shi, Q.Q. Physiological responses of *Phragmites australis* to wastewater with different chemical oxygen demands. *Ecol. Eng.* **2010**, *36*, 1341–1347. [CrossRef]
23. Ong, S.A.; Uchiyama, K.; Inadama, D.; Ishida, Y.; Yamagiwa, K. Performance evaluation of laboratory scale up-flow constructed wetlands with different designs and emergent plants. *Bioresour. Technol.* **2010**, *101*, 7239–7244. [CrossRef] [PubMed]
24. Feng, W.; Xiao, K.; Zhou, W.B.; Zhu, D.W.; Zhou, Y.Y.; Yuan, Y.; Xiao, N.D.; Wan, X.Q.; Hua, Y.M.; Zhao, J.W. Analysis of utilization technologies for Eichhornia crassipes biomass harvested after restoration of wastewater. *Bioresour. Technol.* **2017**, *223*, 287–295. [CrossRef] [PubMed]
25. Bai, F.; Chisholm, R.; Sang, W.G.; Dong, M. Spatial risk assessment of alien invasive plants in China. *Environ. Sci. Technol.* **2013**, *47*, 7624–7632. [CrossRef] [PubMed]
26. Zhou, Q.Y.; Gao, J.Q.; Zhang, R.M.; Zhang, R.Q. Ammonia stress on nitrogen metabolism in tolerant aquatic plant-*Myriophyllum aquaticum*. *Ecotox. Environ. Safe* **2017**, *143*, 102–110. [CrossRef] [PubMed]
27. Liu, F.; Zhang, S.N.; Wang, Y.; Li, Y.; Xiao, R.L.; Li, H.F.; He, Y.; Zhang, M.M.; Wang, D.; Li, X.; et al. Nitrogen removal and mass balance in newly-formed *Myriophyllum aquaticum* mesocosm during a single 28-day incubation with swine wastewater treatment. *J. Environ. Manag.* **2016**, *166*, 596–604. [CrossRef] [PubMed]
28. Ruiz-Rueda, O.; Hallin, S.; Baneras, L. Structure and function of denitrifying and nitrifying bacterial communities in relation to the plant species in a constructed wetland. *FEMS Microbiol. Ecol.* **2009**, *67*, 308–319. [CrossRef] [PubMed]
29. He, S.; Wang, Y.M.; Li, C.S.; Li, Y.C.; Zhou, J. The nitrogen removal performance and microbial communities in a two-stage deep sequencing constructed wetland for advanced treatment of secondary effluent. *Bioresour. Technol.* **2018**, *248*, 82–88. [CrossRef] [PubMed]
30. Cao, Q.Q.; Wang, H.; Chen, X.C.; Wang, R.Q.; Liu, J. Composition and distribution of microbial communities in natural river wetlands and corresponding constructed wetlands. *Ecol. Eng.* **2017**, *98*, 40–48. [CrossRef]
31. Button, M.; Auvinen, H.; Van Koetsem, F.; Hosseinkhani, B.; Rousseau, D.; Weber, K.P.; Du Laing, G. Susceptibility of constructed wetland microbial communities to silver nanoparticles: A microcosm study. *Ecol. Eng.* **2016**, *97*, 476–485. [CrossRef]
32. Du, L.; Chen, Q.R.; Liu, P.P.; Zhang, X.; Wang, H.H.; Zhou, Q.H.; Xu, D.; Wu, Z.B. Phosphorus removal performance and biological dephosphorization process in treating reclaimed water by Integrated Vertical-flow Constructed Wetlands (IVCWs). *Bioresour. Technol.* **2017**, *243*, 204–211. [CrossRef] [PubMed]
33. Ibekwe, A.M.; Grieve, C.M.; Lyon, S.R. Characterization of microbial communities and composition in constructed dairy wetland wastewater effluent. *Appl. Environ. Microbiol.* **2003**, *69*, 5060–5069. [CrossRef] [PubMed]
34. Lloyd, J.R.; Klessa, D.A.; Parry, D.L.; Buck, P.; Brown, N.L. Stimulation of microbial sulphate reduction in a constructed wetland: Microbiological and geochemical analysis. *Water Res.* **2004**, *38*, 1822–1830. [CrossRef] [PubMed]

35. Lv, T.; Zhang, Y.; Carvalho, P.N.; Zhang, L.; Button, M.; Arias, C.A.; Weber, K.P.; Brix, H. Microbial community metabolic function in constructed wetland mesocosms treating the pesticides imazalil and tebuconazole. *Ecol. Eng.* **2017**, *98*, 378–387. [CrossRef]
36. Pollard, P.C. Bacterial activity in plant (*Schoenoplectus validus*) biofilms of constructed wetlands. *Water Res.* **2010**, *44*, 5939–5948. [CrossRef] [PubMed]
37. Ishida, C.K.; Kelly, J.J.; Gray, K.A. Effects of variable hydroperiods and water level fluctuations on denitrification capacity, nitrate removal, and benthic-microbial community structure in constructed wetlands. *Ecol. Eng.* **2006**, *28*, 363–373. [CrossRef]
38. Sun, H.S.; Liu, F.; Xu, S.J.; Wu, S.H.; Zhuang, G.Q.; Deng, Y.; Wu, J.S.; Zhuang, X.L. *Myriophyllum aquaticum* constructed wetland effectively removes nitrogen in swine wastewater. *Front. Microbiol.* **2017**, *8*. [CrossRef] [PubMed]
39. Wang, W.H.; Wang, Y.; Li, Z.; Wei, C.Z.; Zhao, J.C.; Sun, L.Q. Effect of a strengthened ecological floating bed on the purification of urban landscape water supplied with reclaimed water. *Sci. Total Environ.* **2018**, *622*, 1630–1639. [CrossRef] [PubMed]
40. Wang, C.Y.; Sample, D.J. Assessment of the nutrient removal effectiveness of floating treatment wetlands applied to urban retention ponds. *J. Environ. Manag.* **2014**, *137*, 23–35. [CrossRef] [PubMed]
41. Ramprasad, C.; Smith, C.S.; Memon, F.A.; Philip, L. Removal of chemical and microbial contaminants from greywater using a novel constructed wetland: GROW. *Ecol. Eng.* **2017**, *106*, 55–65. [CrossRef]
42. Luo, P.; Liu, F.; Liu, X.L.; Wu, X.; Yao, R.; Chen, L.; Li, X.; Xiao, R.L.; Wu, J.S. Phosphorus removal from lagoon-pretreated swine wastewater by pilot-scale surface flow constructed wetlands planted with *Myriophyllum aquaticum*. *Sci. Total Environ.* **2017**, *576*, 490–497. [CrossRef] [PubMed]
43. Liu, J.Z.; Wang, F.W.; Liu, W.; Tang, C.; Wu, C.X.; Wu, Y.H. Nutrient removal by up-scaling a hybrid floating treatment bed (HFTB) using plant and periphyton: From laboratory tank to polluted river. *Bioresour. Technol.* **2016**, *207*, 142–149. [CrossRef] [PubMed]
44. Wu, Q.; Hu, Y.; Li, S.Q.; Peng, S.; Zhao, H.B. Microbial mechanisms of using enhanced ecological floating beds for eutrophic water improvement. *Bioresour. Technol.* **2016**, *211*, 451–456. [CrossRef] [PubMed]
45. Sun, G.Z.; Saeed, T. Kinetic modelling of organic matter removal in 80 horizontal flow reed beds for domestic sewage treatment. *Process Biochem.* **2009**, *44*, 717–722. [CrossRef]
46. Nguyen, X.C.; Chang, S.W.; Nguyen, T.L.; Ngo, H.H.; Kumar, G.; Banu, J.R.; Vu, M.C.; Le, H.S.; Nguyen, D.D. A hybrid constructed wetland for organic-material and nutrient removal from sewage: Process performance and multi-kinetic models. *J. Environ. Manag.* **2018**, *222*, 378–384. [CrossRef] [PubMed]
47. Saeed, T.; Sun, G.Z. The removal of nitrogen and organics in vertical flow wetland reactors: Predictive models. *Bioresour. Technol.* **2011**, *102*, 1205–1213. [CrossRef] [PubMed]
48. Toscano, A.; Langergraber, G.; Consoli, S.; Cirelli, G.L. Modelling pollutant removal in a pilot-scale two-stage subsurface flow constructed wetlands. *Ecol. Eng.* **2009**, *35*, 281–289. [CrossRef]
49. Weerakoon, G.M.P.R.; Jinadasa, K.B.S.N.; Herath, G.B.B.; Mowjood, M.I.M.; Van Bruggen, J.J.A. Impact of the hydraulic loading rate on pollutants removal in tropical horizontal subsurface flow constructed wetlands. *Ecol. Eng.* **2013**, *61*, 154–160. [CrossRef]
50. Huang, J.; Reneau, R.B.; Hagedorn, C. Nitrogen removal in constructed wetlands employed to treat domestic wastewater. *Water Res.* **2000**, *34*, 2582–2588. [CrossRef]
51. Toet, S.; Van Logtestijn, R.S.P.; Kampf, R.; Schreijer, M.; Verhoeven, J.T.A. The effect of hydraulic retention time on the removal of pollutants from sewage treatment plant effluent in a surface-flow wetland system. *Wetlands* **2005**, *25*, 375–391. [CrossRef]
52. Zhang, S.; Pang, S.; Wang, P.; Wang, C.; Guo, C.; Addo, F.G.; Li, Y. Responses of bacterial community structure and denitrifying bacteria in biofilm to submerged macrophytes and nitrate. *Sci. Rep.* **2016**, *6*, 36178. [CrossRef] [PubMed]
53. Liu, F.; Zhang, S.N.; Luo, P.; Zhuang, X.L.; Chen, X.; Wu, J.S. Purification and reuse of non-point source wastewater via *Myriophyllum*-based integrative biotechnology: A review. *Bioresour. Technol.* **2018**, *248*, 3–11. [CrossRef] [PubMed]
54. Rehman, F.; Pervez, A.; Khattak, B.N.; Ahmad, R. Constructed wetlands: Perspectives of the oxygen released in the rhizosphere of macrophytes. *Clean-Soil Air Water* **2017**, *45*. [CrossRef]
55. Klomjek, P.; Nitisoravut, S. Constructed treatment wetland: A study of eight plant species under saline conditions. *Chemosphere* **2005**, *58*, 585–593. [CrossRef] [PubMed]

56. Mburu, N.; Tebitendwa, S.M.; Rousseau, D.P.L.; Van Bruggen, J.J.A.; Lens, P.N.L. Performance evaluation of horizontal subsurface flow-constructed wetlands for the treatment of domestic wastewater in the tropics. *J. Environ. Eng.* **2013**, *139*, 358–367. [CrossRef]
57. Song, H.L.; Li, X.N.; Lu, X.W.; Inamori, Y. Investigation of microcystin removal from eutrophic surface water by aquatic vegetable bed. *Ecol. Eng.* **2009**, *35*, 1589–1598. [CrossRef]
58. Li, L.F.; Li, Y.H.; Biswas, D.K.; Nian, Y.G.; Jiang, G.M. Potential of constructed wetlands in treating the eutrophic water: Evidence from Taihu Lake of China. *Bioresour.Technol.* **2008**, *99*, 1656–1663. [CrossRef] [PubMed]
59. Katsenovich, Y.P.; Hummel-Batista, A.; Ravinet, A.J.; Miller, J.F. Performance evaluation of constructed wetlands in a tropical region. *Ecol. Eng.* **2009**, *35*, 1529–1537. [CrossRef]
60. Wu, J.; Zhang, J.; Jia, W.L.; Xie, H.J.; Gu, R.R.; Li, C.; Gao, B.Y. Impact of COD/N ratio on nitrous oxide emission from microcosm wetlands and their performance in removing nitrogen from wastewater. *Bioresour. Technol.* **2009**, *100*, 2910–2917. [CrossRef] [PubMed]
61. Ding, Y.; Song, X.S.; Wang, Y.H.; Yan, D.H. Effects of dissolved oxygen and influent COD/N ratios on nitrogen removal in horizontal subsurface flow constructed wetland. *Ecol. Eng.* **2012**, *46*, 107–111. [CrossRef]
62. Zhu, H.; Yan, B.X.; Xu, Y.Y.; Guan, J.N.; Liu, S.Y. Removal of nitrogen and COD in horizontal subsurface flow constructed wetlands under different influent C/N ratios. *Ecol. Eng.* **2014**, *63*, 58–63. [CrossRef]
63. Fu, G.P.; Yu, T.Y.; Ning, K.L.; Guo, Z.P.; Wong, M.H. Effects of nitrogen removal microbes and partial nitrification-denitrification in the integrated vertical-flow constructed wetland. *Ecol. Eng.* **2016**, *95*, 83–89. [CrossRef]
64. Turner, B.L.; Newman, S.; Newman, J.M. Organic phosphorus sequestration in subtropical treatment wetlands. *Environ. Sci. Technol.* **2006**, *40*, 727–733. [CrossRef] [PubMed]
65. Arias, C.A.; Del Bubba, M.; Brix, H. Phosphorus removal by sands for use as media in subsurface flow constructed reed beds. *Water Res.* **2001**, *35*, 1159–1168. [CrossRef]
66. Westholm, L.J. Substrates for phosphorus removal–potential benefits for on-site wastewater treatment? *Water Res.* **2006**, *40*, 23–36. [CrossRef] [PubMed]
67. Caselles-Osorio, A.; Garcia, J. Performance of experimental horizontal subsurface flow constructed wetlands fed with dissolved or particulate organic matter. *Water Res.* **2006**, *40*, 3603–3611. [CrossRef] [PubMed]
68. Ghosh, D.; Gopal, B. Effect of hydraulic retention time on the treatment of secondary effluent in a subsurface flow constructed wetland. *Ecol. Eng.* **2010**, *36*, 1044–1051. [CrossRef]